HHS Public Access

Author manuscript

Int J Biochem Cell Biol. Author manuscript; available in PMC 2018 January 01.

Published in final edited form as:

Int J Biochem Cell Biol. 2017 January ; 82: 28–40. doi:10.1016/j.biocel.2016.11.014.

Inhibition of histone/lysine acetyltransferase activity kills $CoCl_2$-treated and hypoxia-exposed gastric cancer cells and reduces their invasiveness

Suvasmita Rath[a], **Lopamudra Das**[a], **Shrikant Babanrao Kokate**[a], **Nilabh Ghosh**[a], **Pragyesh Dixit**[a], **Niranjan Rout**[b], **Shivaram P. Singh**[c], **Subhasis Chattopadhyay**[a], **Hassan Ashktorab**[d], **Duane T. Smoot**[e], **Mahadeva M. Swamy**[f], **Tapas K. Kundu**[f], **Sheila E. Crowe**[g], and **Asima Bhattacharyya**[a,*]

[a]School of Biological Sciences, National Institute of Science Education and Research (NISER) Bhubaneswar, HBNI, P.O. Bhimpur-Padanpur, Via Jatni, Dist. Khurda, 752050, Odisha, India

[b]Oncopathology, Acharya Harihar Regional Cancer Centre, Cuttack, 753007, Odisha, India

[c]Department of Gastroenterology, SCB Medical College, Cuttack, 753007, Odisha, India

[d]Department of Medicine, Howard University, Washington, DC, 20059, USA

[e]Department of Medicine, Meharry Medical Center, Nashville, TN, 37208, USA

[f]Transcription and Disease Laboratory, Molecular Biology and Genetics Unit, JNCASR, Jakkur PO, Bangalore 560064, Karnataka, India

[g]School of Medicine, University of California, San Diego, CA, 92093, USA

Abstract

Hypoxia enhances immortality and metastatic properties of solid tumors. Deregulation of histone acetylation has been associated with several metastatic cancers but its effect on hypoxic responses of cancer cells is not known. This study aimed at understanding the effectiveness of the hydrazinocurcumin, CTK7A, an inhibitor of p300 lysine/histone acetyltransferase (KAT/HAT) activity, in inducing apoptosis of gastric cancer cells (GCCs) exposed to cobalt chloride ($CoCl_2$), a hypoxia-mimetic chemical, or 1% O_2. Here, we show that CTK7A-induced hydrogen peroxide (H_2O_2) generation in $CoCl_2$-exposed and invasive gastric cancer cells (GCCs) leads to p38 MAPK-mediated Noxa expression and thereafter, mitochondrial apoptotic events. Noxa induction in normal immortalized gastric epithelial cells after CTK7A and hypoxia-exposure is remarkably less in comparison to similarly-treated GCCs. Moreover, hypoxia-exposed GCCs, which have acquired invasive properties, become apoptotic after CTK7A treatment to a significantly higher extent than normoxic cells. Thus, we show the potential of CTK7A in sensitizing hypoxic and metastatic GCCs to apoptosis induction.

*Corresponding author. asima@niser.ac.in (A. Bhattacharyya).

Competing interests

The authors declare that they have no competing interests.

Appendix A. Supplementary data

Supplementary data associated with this article can be found, in the online version, at http://dx.doi.org/10.1016/j.biocel.2016.11.014.

Keywords

Apoptosis; Cancer metastasis; CTK7A; HAT; Hif1α; Hypoxia

1. Introduction

Solid tumors are different from normal tissues in terms of their oxygen supply and consumption. The core of solid tumors become hypoxic due to inefficient blood supply (Karakashev and Reginato, 2015; Rankin and Giaccia, 2008). Hypoxia provides the ideal microenvironment for promoting metastasis (Sullivan and Graham, 2007). Naturally, like other solid tumors, gastric cancer malignancy and treatment resistance are largely, if not solely, determined by hypoxia (Vaupel and Mayer, 2007). Thus, selective therapeutic targeting of hypoxic metastatic gastric cancer cells is a challenging area of research.

Hypoxic cells undergo several hypoxia-adaptations. The master regulatory protein expressed in hypoxic cells is hypoxia-inducible factor1 (Hif1). Hif1 is a heterodimeric protein having two subunits, α and β. While Hif1α gets degraded in normoxia and hypoxia stabilizes it, Hif1β is constitutively expressed and its stability is not regulated by cellular oxygenation status (Huang et al., 1998). Hif1α dimerizes with Hif1β and transcriptionally activates a number of hypoxia-responsive genes by binding to the hypoxia-responsive elements (HREs) (Rohwer et al., 2009). p300 acts as a transcriptional coactivator of Hif1. p300 has an intrinsic histone or lysine (K) acetyltransferase (HAT or KAT) activity and functions as a protein scaffold (Chan and La Thangue, 2001; Santer et al., 2011). Autoacetylation induces acetyltransferase activity of p300. Both enhanced and suppressed (HAT) activity in tumor cells can lead to cell cycle arrest and apoptosis (Clarke et al., 1999; Kawamura et al., 2004). It is evident from the literature that the relation of HAT activity with cancer is tissue and context-dependent. Dysregulation of histone acetylation and deacetylation have been associated with gastric cancer progression and invasiveness (Yang et al., 2014). Studies have found expression of Hif1α in gastric cancer and have associated Hif1α with aggressive metastasis and treatment resistance (Liu et al., 2008; Rohwer and Cramer, 2010; Urano et al., 2006). Induction of apoptotic cell death in invasive cancer cells is a highly desired goal to achieve for cancer therapists. Cellular apoptosis is orchestrated by two separate signaling pathways- the mitochondria-mediated intrinsic pathway and the death receptor-mediated extrinsic pathway (Cotter, 2009). Chemo and radiotherapy induce the former pathway by involving the Bcl2 family proteins. A Bcl2 homology 3 (BH3)-only tumor suppressor protein Noxa is transcriptionally induced by Hif1 and induces mitochondria mediated intrinsic apoptotic pathway (Gomez-Bougie et al., 2011).

In this study, we investigated the role of p300 HAT activity on Noxa-mediated apoptosis in $CoCl_2$-treated and 1% O_2-exposed GCCs. We showed that downregulation of HAT activity significantly induced reactive oxygen species (ROS) generation as well as Noxa-mediated apoptosis selectively in hypoxic GCCs but not in non-hypoxic GCCs. In addition, the expression of metastatic markers in $CoCl_2$-treated GCCs was also downregulated after suppression of HAT activity by the hydrazinocurcumin, CTK7A. Thus, this study revealed a

previously undescribed mechanism for how CTK7A can induce apoptosis in hypoxia-exposed invasive GCCs and further enriched our understanding of its antitumor effects.

2. Methods

2.1. Cell lines

GCCs AGS, MKN 45, KATO III were cultured and maintained as previously described (Bhattacharyya et al., 2009). Immortalized human GCC cell HFE145 and pDsRed2 (Clontech, CA, USA)-expressing AGS stable cells were maintained in 10% heat-inactivated FBS-supplemented RPMI 1640. Most of the studies were performed using non-metastatic AGS cells so that metastasis induction could be clearly identified. HFE145 cells were used to study properties of non-malignant human gastric epithelial cells. *hif1α* knockdown cells were prepared as described previously (Rath et al., 2015).

2.2. Chemicals and reagents

Cobalt chloride hexahydrate ($CoCl_2 \cdot 6H_2O$) (Sigma-Aldrich, MO, USA) or 1% O_2 was used to induce hypoxia in AGS cells as per standard methods (Rath et al., 2016; Wu and Yotnda, 2011). CTK7A at 100 μM dose (Arif et al., 2010) either alone or in combination with $CoCl_2$ (200 μM) was used for 24 h treatment. ERK1/2 inhibitor PD98059, p38 MAPK inhibitor SB203580, and JNK inhibitor IISP600125 (all from Calbiochem, CA, USA) were used at 25 μM dose for 1 h prior to $CoCl_2$ and CTK7A treatment. Superoxide dismutase (SOD) and catalase (CAT) (both from Sigma Aldrich) were used at 200 units/ml and 350 units/ml dose, respectively, for 4 h prior to treatment with $CoCl_2$ and CTK7A. 5-(and 6)-chloromethyl-2,7-dichlorodihydrofluorescein diacetate, acetyl ester (CM-H_2-DCFDA; Invitrogen, CA, USA) was used to detect intracellular ROS generation.

2.3. Whole cell, nuclear, cytosolic and mitochondrial lysate preparation

Whole cell lysates were prepared by standard protein isolation protocol. Nuclear and cytoplasmic fractions were isolated using NE-PER Kit following manufacturer's instruction (Thermo Scientific, IL, USA). Mitochondrial lysates were prepared following a previously-described protocol (Rath et al., 2015).

2.4. Western blots, antibodies and immunoprecipitation

Proteins were separated by sodium dodecyl sulphate polyacrylamide gel electrophoresis (SDS-PAGE) followed by western blotting. Membranes were probed with specific antibodies for p300, acetylated lysine, Hif1α, Noxa, Twist1 (Abcam, MA, USA), caspase 3, caspase 9, Cytochrome *c*, N cadherin, E cadherin, phospho p38 MAPK, phospho ERK and phospho JNK (Cell Signaling Technology, MA, USA). GAPDH (Imgenex Corporation, CA, USA) and Cox IV (Cell Signaling Technology, MA, USA) antibodies were used as loading controls for the cytosolic fraction and mitochondrial fractions, respectively. Proteins were detected by using Super Signal West Femto kit (Thermo scientific). Images were taken with Chemidoc XRS (Bio-Rad Laboratories, CA, USA) equipped with Quantity One-4.6.9 software.

2.5. Flow cytometry

Apoptosis was quantified by flow cytometry. AGS cells were treated with $CoCl_2$ (Sigma-Aldrich) alone and/or CTK7A for 24 h or left untreated. Cell pellets were washed twice with chilled PBS and stained with Annexin V PE/7-AAD (BD Biosciences, CA, USA) according to manufacturer's instruction. 1×10^4 cells were acquired per sample using FACSCalibur Flow Cytometer (BD Biosciences). Results were analyzed by CellQuest Pro software (BD Biosciences).

2.6. Confocal microscopy

pDsRed2 (Clontech)-expressing AGS stable cells were used for confocal microscopy. These cells were treated with $CoCl_2$ and/or CTK7A or left untreated for 24 h. Noxa translocation to mitochondria and cytochrome *c* release from mitochondria were studied in the above experimental condition. Cells were fixed with 4% paraformaldehyde at 37°C for 15 min followed by incubation with DAPI (4′, 6-Diamidino-2-Phenylindole, Dilactate (Invitrogen) for 20 min. Mitochondrial morphology was studied as described earlier (Rath et al., 2015). Fragmentation of mitochondria, as assessed by roundness, circularity and length, was measured by ImageJ software (NIH, MD, USA). Roundness [4 × (surface area)/(π × major axis^2)] and circularity [4π × (surface area/perimeter^2)] together represented mitochondrial sphericity (sphericity value 1 = perfect spheroid).

2.7. Transwell migration and invasion assay

Cell migration and invasion assays were performed using 8-μm pore size Transwell Biocoat control inserts (migration assay) or matrigel-coated inserts, as per manufacturer's instruction (Becton Dickinson, MA, USA). 5×10^4 AGS cells in serum free media were seeded on the upper surface of 24 well transwell plate and 10% FBS-containing media was added to the lower chamber. Cells were treated with $CoCl_2$ or 1% O_2 alone and/or CTK7A for 24 h or left untreated. After completion of the incubation, upper surfaces of transwell were scraped off and cells in the lower surface were fixed for 30 min with 4% paraformaldehyde, and stained for 30 min with haematoxylin. Migrated and invaded cells were counted (from five different fields) under an inverted microscope (Primo Vert, Carl Zeiss, Jena, Germany).

2.8. Wound healing assay

1×10^6 AGS cells were seeded in 35 mm plates and wound healing assays were performed as described earlier were kept for 24 h to create a monolayer of cells. Multiple uniform wounds of constant diameter were made on the monolayer culture. Detached cells were washed followed by 24 h treatment of $CoCl_2$ and/or CTK7A or were left untreated. Imaging was done by an inverted microscope equipped with camera (Primo Vert, Carl Zeiss).

2.9. Soft agar assay

AGS cells were harvested and 1×10^3 cells were mixed with 0.3% top agar and plated onto 0.6% bottom agar in 6 cm cell culture plates. Cells were treated with $CoCl_2$ (50 μM) and/or CTK7A (100 μM) for 24 h. These plates were fed twice weekly with the above treatment condition and maintained for 3 weeks in a humidified incubator containing 5% CO_2. At the

end of the incubation period, visible colonies on the top agar were directly counted and colony sizes were compared between various treatment groups.

2.10. Human gastric biopsy specimen collection and florescence microscopy

Biopsy samples from the antral gastric mucosa were collected from patients suffering from metastatic gastric cancer and undergoing diagnostic esophagogastroduodenoscopy following a National Institute of Science Education and Research (NISER) Review Board-approved protocol. Written informed consent was obtained from all patients. Gastric biopsy samples were embedded in optimal cutting temperature (OCT) compound (VWR International, Lutterworth, UK). Cryosectioning was performed at 10 μm (Leica, Wetzlar, Germany). Sections were stained with Hif1α, Twist1, E-cadherin and N-cadherin primary antibodies followed by incubation with fluorescently labelled secondary antibodies (Alexa Fluor 488 anti-rabbit and anti mouse from Molecular Probes, Invitrogen, Paisley). The sections were examined by a fluorescence microscope (Olympus, Tokyo, Japan).

2.11. Reactive oxygen species (ROS) measurement

ROS was measured by staining cells with a membrane-permeable dye, 5-(and 6)-chloromethyl-2,7-dichlorodihydrofluorescein diacetate, acetyl ester (CM-H_2-DCFDA; Invitrogen). 0.166×10^6 AGS cells were grown on 9 mm coverslips in 24 well cell culture plates. After treatment, cells were stained with 1 μM CM-H_2-DCFDA and incubated for 10 min at 37°C in the dark. Cells were fixed with 4% paraformaldehyde for 10 min at room temperature and viewed by fluorescence microscope (Olympus).

2.12. Statistics

Values are given as mean ± SEM. Student's *t*-test was performed for comparison between groups. Statistical significance was determined at $P < 0.05$. 2-way ANOVA was performed to compare various transfected groups. Bonferroni test was applied for *post hoc* analysis. Colocalization analysis of confocal images was performed by ImageJ plugin Coloc 2.

3. Results

3.1. $CoCl_2$ and 1% O_2 treatment enhances expression of metastatic factors in AGS cells

Cobalt chloride ($CoCl_2$) mimics hypoxia, induces ROS generation and promotes mitochondria-mediated apoptosis (Torii et al., 2011; Wang et al., 2000). $CoCl_2$ has the same biochemical response as that of physiological hypoxia (Bae et al., 2012; Lee et al., 2001) and induces Hif1α expression in GCCs (Rath et al., 2016). In contrast, several reports have also shown that $CoCl_2$-induced Hif1α inhibits apoptosis (Piret et al., 2005, 2002) and enhances metastatic potential (Zhang et al., 2013). In order to study the expression of metastatic factors in GCCs after treatment with 200 μM cobalt chloride hexahydrate ($CoCl_2 \cdot 6H_2O$) for various time periods, western blotting were performed. Although *GAPDH* is a Hif1-target gene, we used GAPDH as a loading control since GAPDH was not found to be regulated by hypoxia in the gastric cancer cell lines AGS (Xiao et al., 2012), MGS-803 and SGC-7901 (Luo et al., 2010) as well as in other hypoxic cancer cells studied *in vitro* (Jung et al., 2014; Said et al., 2007, 2009). Western blot data (n = 3) showed that although Hif1α was significantly induced as early as 3 h of treatment and it was maintained up to 24

h, Hif1α-dependent metastasis-inducing transcription factor Twist1 was noticeably enhanced only at 12 and 24 h of $CoCl_2$ treatment (Fig. 1A). The mesenchymal marker N-cadherin was highly upregulated at 24 h of $CoCl_2$ treatment. Therefore, we used 200 μM $CoCl_2$ and 100 μM CTK7A [(Sodium 4-(3, 5-bis (4-hydroxy-3-methoxystyryl)-1H-pyrazol-1-yl) benzoate], a curcumin-derived water soluble HAT/KAT and p300 autoacetylation inhibitor treatment for 24 h for the rest of our experiments. As AGS cells do not express the invasion-suppressor epithelial marker E-cadherin (Oliveira et al., 2009), we did not observe the other component of "cadherin switch" associated with metastasis, the E-cadherin degradation (Gheldof and Berx, 2013) in $CoCl_2$-treated hypoxic AGS cells. p300, however, remained equally expressed at all time points. We also performed immunofluorescence microscopy on human metastatic gastric cancer biopsies and compared with matched controls from adjacent noncancerous areas. Metastatic samples (n = 4), which showed substantial high expression of Hif1α, also had high Twist1 and N-cadherin but showed much lower E-cadherin expression compared to their matched controls (n = 4) (Fig. S1A).

In an attempt to understand the effect of HAT function inhibition on the expression of Hif1α and the above-mentioned metastasis markers, AGS cells were incubated for 24 h with 100 μM of CTK7A in the presence or absence of 200 μM $CoCl_2$ or were left untreated. Western blotting (n = 3) of whole cell lysates showed that $CoCl_2$-mediated induced expression of Hif1α, Twist1 and N-cadherin was substantially inhibited by CTK7A (Fig. 1B). We also noticed that acetylated p300 (ac-p300) remained suppressed in $CoCl_2$ plus CTK7A-treated cells as compared to the other three treatment groups. p300 expression was not altered by CTK7A treatment. Twist1 and N-cadherin expression in CTK7A-treated and untreated $CoCl_2$-exposed AGS cells were further assessed by confocal microscopy (n = 3) (Fig. S1B). Confocal images complemented our findings shown in Fig. 1B. As protein expression varies from cell to cell, we tested Hif1α, N-cadherin and Twist1 expression in $CoCl_2$ and CTK7A-treated MKN45 and Kato III cells. Data (n = 3) confirmed that as in AGS cells, $CoCl_2$-induced expression of Hif1α, N-cadherin and Twist1 in MKN45 and Kato III cells was significantly inhibited by CTK7A treatment (Figs. 1C and S2A). To study the effect of CTK7A in hypoxic environment, GCCs were exposed to normoxia (21% O_2) and hypoxia (1% O_2) for 24 h in the presence or absence of CTK7A. Whole cell lysates were immunoblotted (n = 3) to detect the expression of EMT markers. CTK7A showed the same effect on Hif1α, N-cadherin and Twist1 expression in 1% O_2–treated cells as it was found in $CoCl_2$-treated cells (Figs. 1D and S2B). Therefore, majority of our experiments were performed using $CoCl_2$ unless we stated specifically about treating cells with 1% O_2.

3.2. CTK7A decreases migration and invasion properties in $CoCl_2$ as well as 1% O_2-treated GCCs

Hypoxia plays a positive role in gastric cancer invasion and migration (Xing et al., 2011; Zhong et al., 1999). In order to assess the effect of HAT inhibition on migrating ability of hypoxic GCCs, we performed transwell migration assay and wound healing assay. Cells were seeded in inserts for transwell migration assay and were treated with CTK7A and $CoCl_2$ or 1% O_2 for 24 h. Migrated cells were stained with hematoxylin and studied under a microscope. A significant reduction in hypoxia-induced migration was observed upon CTK7A treatment (Fig. 2A and B) (n = 4, $*P < 0.05$). For further validation of our data,

wound healing assay was performed. Confluent layers of AGS cells were wounded and exposed to CTK7A and $CoCl_2$. After 24 h, we found that control and only CTK7A-treated cells were comparable to $CoCl_2$ and CTK7A-treated cells with respect to their poor wound-healing ability but $CoCl_2$-treated cells had significantly high (n = 4, *P < 0.05) wound-healing ability than other groups (Fig. S3A). Invasiveness of GCCs was measured by matrigel invasion assay which showed significant (n = 4, $*P < 0.05$) reduction of invasive property in hypoxia plus CTK7A-treated GCCs as compared to only hypoxia exposed cells (Fig. 2C and D). The change in clonogenic potential of $CoCl_2$-treated AGS cells after CTK7A treatment was examined by soft agar assay (n = 3). We found that the number of foci was significantly ($*P < 0.05$, $**P < 0.01$, $***P < 0.001$) increased by $CoCl_2$ exposure as compared to control cells, CTK7A plus $CoCl_2$-exposed cells showed significantly less foci formation than only $CoCl_2$-treated cells (Fig. S3B).

3.3. Inhibition of HAT activity induces Noxa in hypoxic GCCs in a Hif1α-independent manner

Hif1α depletion in gastric cancer cell line induces apoptosis under hypoxia (Tanaka et al., 2015). Noxa is a mediator of apoptosis in hypoxic cells and is induced by Hif1α (Kim et al., 2004). In an attempt to assess Noxa expression pattern in hypoxic cells, AGS cells were treated with 200 μM $CoCl_2$ for 3 h, 12 h and 24 h. Western blot data (n = 3) revealed a time-dependent enhancement in Noxa expression in $CoCl_2$-treated cells ($*P < 0.05$) (Fig. 3 A). We next assessed Noxa expression in control and $CoCl_2$-treated AGS cells with or without CTK7A treatment by performing western blotting (n = 3) of whole cell lysates. Although CTK7A and $CoCl_2$ independently induced Noxa expression, CTK7A treatment resulted in a far higher ($*P < 0.05$) Noxa expression in $CoCl_2$-treated cells than in untreated cells (Fig. 3B). Treatment of normal immortalized HFE145 cells with CTK7A showed a much lower magnitude of Noxa induction in CTK7A plus $CoCl_2$-treated cells than their AGS counterparts (Fig. 3C). MKN45 and KATO III cells, two other GCCs with metastatic properties, were also tested for their Noxa expression pattern. Noxa expression in these cells showed the same trend as in AGS cells (n = 3, $*P < 0.05$) (Fig. 3D). In order to assess Noxa expression by hypoxia and CTK7A, AGS cells were exposed to normoxia and hypoxia (1% O_2) in the presence or absence of CTK7A. Noxa expression was significantly high in CTK7A and 1% O_2 co-treated cells as compared to only 1% O_2-treated cells (Fig. 3E). Noxa expression is known to be induced by the transcription factor Hif1. Our data always showed significantly high Hif1α expression in only $CoCl_2$ (or 1% O_2)-exposed GCCs as compared to $CoCl_2$ (or 1% O_2) and CTK7A-treated cells (Fig. 1B, C, E and F). Noxa expression was always high in $CoCl_2$ (or 1% O_2) and CTK7A-treated GCCs as compared to only $CoCl_2$ (or 1% O_2)-treated hypoxic GCCs (Fig. 3C–F). To find out the role of Hif1α on Noxa expression in the presence of CTK7A, AGS cells were stably transfected with Hif1α shRNA (Rath et al., 2015). The knockdown of Hif1α significantly suppressed $CoCl_2$-mediated Hif1α protein expression than empty vector and scrambled shRNA-expressing cells but did not change the pattern of CTK7A-induced Noxa expression in $CoCl_2$-treated AGS cells. These data confirmed that Noxa regulation in hypoxic CTK7A-treated GCCs was not dependent on Hif1α (Fig. 3F).

3.4. CTK7A induces mitochondrial translocation of Noxa and intrinsic apoptosis events in hypoxic GCCs

Since mitochondrial translocation of Noxa is required for its apoptotic activity (Lowman et al., 2010; Rath et al., 2015), we examined mitochondrial Noxa status after CTK7A treatment. Western blotting (n = 3) of mitochondrial and cytoplasmic fractions of AGS cells showed significantly higher (*$P < 0.05$) mitochondrial expression and localization of Noxa in CTK7A plus $CoCl_2$-treated cells as compared to control, only CTK7A-treated or only $CoCl_2$-treated cells (Fig. 4A). Confocal microscopy (n = 4) of the same set of cells (Fig. 4B) corroborated western blot results. As cytochrome *c* (Cyt *c*) release is the hallmark of the intrinsic apoptotic pathway, we examined mitochondrial Cyt *c* status before and after CTK7A and $CoCl_2$ treatment. For this, AGS cells stably expressing pDsRed2 were treated with CTK7A and $CoCl_2$ or left untreated. Results (n = 4) clearly indicated that mitochondrial retention of Cyt *c* was drastically reduced in CTK7A plus $CoCl_2$-treated cells (indicating maximal Cyt *c* release into the cytosol) while control cells, CTK7A-treated and $CoCl_2$-treated cells were able to retain mostly all their Cyt *c* in the mitochondria (Fig. 4C). Colocalization analysis of Noxa-pDSRed2 and Cyt *c*-pDSRed2 were performed and the data (Figs. S4A and S4B, respectively) showed significantly high Noxa but significantly less Cyt *c* in the CTK7A + $CoCl_2$-treated mitochondria as compared to the other three treatment groups (n = 4, *$P < 0.05$). These data clearly showed that CTK7A + $CoCl_2$ treated cells were undergoing maximal apoptotic stress. During intrinsic apoptosis, mitochondria undergo fragmentation (appears spheroidal/punctated) before releasing Cyt *c* into the cytosol. Confocal microscopy was performed to find out whether any mitochondrial stress was induced by CTK7A treatment. pDsRed2 stably-expressing AGS cells were treated with CTK7A in the presence or absence of $CoCl_2$. The tubular network of healthy mitochondria observed in control and $CoCl_2$-treated cells was found to be damaged in cells treated with CTK7A. However, mitochondria appeared significantly (n = 4, *$P < 0.05$, **$P < 0.001$) smaller, disintegrated and had increased roundness and circularity in CTK7A plus $CoCl_2$-treated cells when compared with other treatment groups (Fig. S5A and S5B).

Next, we sought to examine the expression of caspase 9, a key factor representing the intrinsic apoptotic pathway and the down-stream effector caspase 3 in relation to Noxa expression. Western blotting (n = 3) of total cell lysates showed that $CoCl_2$ or 1% O_2 plus CTK7A-treated cells had maximal expression of cleaved caspase 9 and cleaved caspase 3 (17, 19 kDa) indicating that these cells were undergoing apoptotic cell death to the greatest extent (Fig. 4D). Graphical representation of Noxa and cleaved caspase 3 (the catalytically active 17 kDa form) identified significantly high expression of these two factors in $CoCl_2$ or 1% O_2 plus CTK7A-treated cells as compared to the other treatment groups (n = 3,*$P < 0.05$), The degree of apoptosis induction in CTK7A plus $CoCl_2$-treated AGS cells was next determined. To detect apoptotic cells, control, $CoCl_2$-treated, CTK7A alone and CTK7A plus $CoCl_2$-treated AGS cells were stained with Annexin V-PE and necrotic population was determined by 7-AAD staining (n = 4). Flow cytometric analysis of the lower-right quadrant showed that CTK7A plus $CoCl_2$-treated cells underwent significantly higher cell death (*$P < 0.05$) compared to the control, CTK7A-treated and only $CoCl_2$-treated cells (Fig. 4E). These data altogether confirmed that CTK7A was a potent inducer of apoptosis selectively in $CoCl_2$ and CTK7A-treated GCCs.

3.5. CTK7A-mediated Noxa induction in $CoCl_2$-treated GCCs is mediated by H_2O_2 generation

Earlier reports correlated HAT activity with ROS generation (Kang et al., 2005). Curcumin, at low concentration, was shown to exert anticancer activity in leukemia by decreasing ROS generation whereas at high dose it killed cells through more ROS production (Chen et al., 2005). As CTK7A was derived from curcumin, we sought to assess the effect of CTK7A on ROS generation. To find out the involvement of superoxide ($O_2^{\bullet-}$) in Noxa induction, we performed western blotting (n = 3) using AGS cell lysates prepared from control cells, only CTK7A-treated cells, $CoCl_2$-treated cells or CTK7A + $CoCl_2$-treated cells in the presence or absence of 200 units/ml superoxide-dismutase (SOD). (−)SOD group and (+)SOD group showed no difference in Hif1α and Noxa expression which indicated that neither CTK7A nor $CoCl_2$ alone or in combination had any role on $O_2^{\bullet-}$ generation (Fig. 5A). In contrast, a 4 h pre-treatment of cells with 350 units/ml of catalase, a H_2O_2 scavenger, markedly suppressed Noxa expression induced by CTK7A + $CoCl_2$ treatment (*$P < 0.05$) (Fig. 5B) while catalase had no suppressive effect on Hif1α expression (n = 3). Chloromethyl-H_2DCFDA (CM-H_2DCFDA) was used at a dose of 1 μM for 10 min to visualize ROS generation in GCCs after CTK7A and $CoCl_2$ treatment. Fluorescence microscopy revealed that although CTK7A or $CoCl_2$ slightly induced ROS generation compared to control (Fig. 5C), CTK7A + $CoCl_2$ treatment induced maximal ROS generation. Pretreatment with catalase notably scavenged that effect. These results suggested that H_2O_2, but not $O_2^{\bullet-}$, was the main mediator in CTK7A-induced Noxa expression in $CoCl_2$-treated AGS cells.

3.6. CTK7A-induced H_2O_2 generation in $CoCl_2$-treated GCCs causes p38 MAPK-mediated Noxa upregulation

Our data established that CTK7A in $CoCl_2$ or 1% O_2-exposed cells caused Noxa-mediated cell death. It is known that ROS can mediate Noxa induction (Fischer et al., 2005) and MAPK activation (Bae et al., 2006; Chung et al., 2013; Liang et al., 2014). In order to find out the effect of H_2O_2 on MAPK activation, we treated AGS cells with catalase prior to treatment with $CoCl_2$ and CTK7A. Whole cell lysates were prepared and western blot data (n = 3) revealed that $CoCl_2$ plus CTK7A-treatment induced maximal JNK, p38 MAPK as well as ERK1/2 phosphorylation compared to control, CTK7A alone or $CoCl_2$-alone (Fig. 6A). Catalase had no suppressive effect on ERK phosphorylation; JNK phosphorylation was partially suppressed and p38 MAPK phosphorylation was noticeably decreased in CTK7A plus $CoCl_2$-treated cells as compared to other treatment groups. This data provided an important direction that p38 MAPK and JNK were mediating Noxa induction in CTK7A and $CoCl_2$-cotreated cells. To find out the role of JNK and p38 MAPK activation on CTK7A-mediated Noxa induction in $CoCl_2$-treated cells, AGS cells were pretreated with SP600125 and SB203580, respectively. Data (n = 3) revealed that JNK inhibition had no effect on Noxa (Fig. 6B) butp38 MAPK inhibition drastically reduced Noxa and the downstream effector molecule, cleaved caspase 3 in CTK7A and $CoCl_2$-treated cells. (Fig. 6C). Altogether, we established that HAT inhibition in $CoCl_2$-treated cells induced Noxa expression which was triggered by ROS-mediated p38 MAPK activation.

4. Discussion

Hypoxic regions remain scattered inside solid tumors as a resultant effect of heterogeneous angiogenesis and poor blood supply to certain parts of the tumor. Cancer cells thrive and progress towards malignancy in hypoxic environments (Vaupel, 2004). Hypoxic cancer cells metastasize very aggressively and become treatment-resistant (Kitajima and Miyazaki, 2013; Lin et al., 2008). The novelty of this work lies in the finding that CTK7A, a hydrazinocurcumin compound, selectively kills hypoxia-exposed and $CoCl_2$-treated GCCs but spares non-hypoxic and $CoCl_2$-untreated cells from apoptotic death to a significant extent. Cancer cells generally are under oxidative stress and further increment in ROS by therapeutic attempts make cancer cells susceptible to ROS-induced cell-damages. Gastric cancer tissues express significant amount of ROS (Bhattacharyya et al., 2014) and therefore, therapeutic interventions of gastric cancer also exploits the ROS-generating machinery (Chen et al., 2008; Matsunaga et al., 2010). This study confirms that CTK7A treatment produces substantially higher amount of ROS in hypoxic cells than in untreated GCCs. Our finding is supported by few other reports which state induced ROS generation in hypoxic cells (Clanton, 2007; Sabharwal and Schumacker, 2014). As $CoCl_2$ also induces ROS generation (Guan et al., 2015) and acts as a chemical hypoxia-inducer (Rath et al., 2016), its role in ROS generation in p300 HAT inhibitor treated cells might have a good therapeutic advantage. Enhanced ROS in $CoCl_2$ plus CTK7A-treated cells induce p38 MAPK-mediated Noxa expression. Noxa translocation to mitochondria significantly increases mitochondrial apoptosis in $CoCl_2$ and CTK7A-cotreated cells. Further, we show that Noxa induction in $CoCl_2$ and CTK7A-co-treated GCCs is dependent on ROS generation. Our analysis also demonstrates that the fold change in Noxa enhancement in hypoxic CTK7A-treated GCCs over the CTK7A-untreated hypoxic cells is much higher than the fold change noticed in their counterparts in non-cancer GCCs. This study further confirms that Noxa induction after CTK7A treatment in hypoxic AGS cells is no longer dependent on Hif1α. This enigma is solved by the finding that Noxa is only slightly induced in $CoCl_2$-treated cells but the upregulation of Noxa following CTK7A treatment in those cells is mostly induced by H_2O_2. This is in keeping with earlier studies which reported about enhanced apoptosis in ROS-generating cells. Cisplatin-mediated ROS induction has been associated with JNK activation and apoptosis of various types of cells including GCCs (Bae et al., 2006). Curcumin-mediated ROS induction reportedly induced JNK signaling and caused apoptosis of human GCCs (Liang et al., 2014). Similar reports exist for ROS-mediated p38 MAPK activation (Chung et al., 2013). The importance of histone acetylation in cancer progression and therapy has been well documented. Suppression of HAT activity of p300 by CTK7A was earlier shown to substantially reduce the xenografted oral cancer progression in mice (Arif et al., 2010). Thus, our finding of ROS and p38 MAPK-mediated enhancement of Noxa expression mostly in HAT activity-suppressed $CoCl_2$-treated cells adds a new layer of complexity to the existing understanding on the altered nature of hypoxic cells and offers hope that even hypoxic cells that show metastatic properties can be killed by CTK7A. Although our study provides important information that ROS and p38 MAPK control CTK7A treatment-induced apoptosis of $CoCl_2$-treated cells, the complete signaling mechanism of ROS upregulation by HAT inhibition remains elusive.

Altogether, our study elaborates the mechanism of p300 hypoacetylation-mediated antitumor activity in $CoCl_2$-treated and hypoxic GCCs. The effectiveness of CTK7A in enhancing Noxa-mediated apoptosis via ROS generation and p38 MAPK activation in hypoxic and invasive GCCs supports the possibility that CTK7A may be further exploited for therapeutic purposes. This has further implications since CTK7A shows the promise to avoid widespread toxicity and serious side effects that are commonly associated with cancer therapy. Future studies are required to confirm the effect of CTK7A on other types of cancer.

Supplementary Material

Refer to Web version on PubMed Central for supplementary material.

Acknowledgments

This work was supported by Fast Track Grant SR/FT/LS-38/2010, Science and Engineering Research Board, Govt. of India, to AB; an Indian Council of Medical Research (ICMR) fellowship to SR; fellowships from Department of Atomic Energy (DAE), India, to LD, SBK and PD. The authors thank Mr. Alok Kumar Jena for his assistance in confocal microscopy.

Abbreviations

Ac	acetylated
BH3	Bcl2 homology 3
CM-H_2-DCFDA	5-(and 6)-chloromethyl-2,7-dichlorodihydrofluorescein diacetate acetyl ester
$CoCl_2 \cdot 6H_2O$	cobalt chloride hexahydrate
Cyt *c*	cytochrome *c*
DAPI	(4′,6-Diamidino-2-phenylindole Dilactate
ERK	extracellular signal-regulated kinases
GCC	gastriccancer cell
HAT	histone acetyltransferase
H_2O_2	hydrogen peroxide
Hif1	hypoxia-inducible factor 1
HRE	hypoxia-responsive element
IP	immunoprecipitation
JNK	c-Jun N-terminal kinase
MAPK	mitogen-activated protein kinase
PAGE	polyacrylamide gel electrophoresis

ROS	reactive oxygen species
SDS	sodium dodecylsulphate
SOD	superoxide dismutase
WT	wild type

References

Arif M, Vedamurthy BM, Choudhari R, Ostwal YB, Mantelingu K, Kodaganur GS, Kundu TK. Nitric oxide-mediated histone hyperacetylation in oral cancer: target for a water-soluble HAT inhibitor CTK7A. Chem. Biol. 2010; 17(8):903–913. [PubMed: 20797619]

Bae IH, Kang SW, Yoon SH, Um HD. Cellular components involved in the cell death induced by cisplatin in the absence of p53 activation. Oncol. Rep. 2006; 15(5):1175–1180. [PubMed: 16596182]

Bae S, Jeong HJ, Cha HJ, Kim K, Choi YM, An IS, Koh HJ, Lim DJ, Lee SJ, An S. The hypoxia-mimetic agent cobalt chloride induces cell cycle arrest and alters gene expression in U266 multiple myeloma cells. Int. J. Mol Med. 2012; 30(5):1180–1186. [PubMed: 22941251]

Bhattacharyya A, Chattopadhyay R, Burnette BR, Cross JV, Mitra S, Ernst PB, Bhakat KK, Crowe SE. Acetylation of apurinic/apyrimidinic endonuclease-1 regulates Helicobacter pylori-mediated gastric epithelial cell apoptosis. Gastroenterology. 2009; 136(7):2258–2269. [PubMed: 19505426]

Bhattacharyya A, Chattopadhyay R, Mitra S, Crowe SE. Oxidative stress: an essential factor in the pathogenesis of gastrointestinal mucosal diseases. Physiol. Rev. 2014; 94(2):329–354. [PubMed: 24692350]

Chan HM, La Thangue NB. p300/CBP proteins: HATs for transcriptional bridges and scaffolds. J. Cell Sci. 2001; 114(Pt. 13):2363–2373. [PubMed: 11559745]

Chen J, Wanming D, Zhang D, Liu Q, Kang J. Water-soluble antioxidants improve the antioxidant and anticancer activity of low concentrations of curcumin in human leukemia cells. Pharmazie. 2005; 60(1):57–61. [PubMed: 15700780]

Chen W, Zhao Z, Li L, Wu B, Chen SF, Zhou H, Wang Y, Li YQ. Hispolon induces apoptosis in human gastric cancer cells through a ROS-mediated mitochondrial pathway. Free Radic. Biol. Med. 2008; 45(1):60–72. [PubMed: 18423410]

Chung KS, Han G, Kim BK, Kim HM, Yang JS, Ahn J, Lee K, Song KB, Won M. A novel antitumor piperazine alkyl compound causes apoptosis by inducing RhoB expression via ROS mediated cAbl/p38 MAPK signaling. Cancer Chemother. Pharmacol. 2013; 72(6):1315–1324. [PubMed: 24121479]

Clanton TL. Hypoxia-induced reactive oxygen species formation in skeletal muscle. J. Appl. Physiol. 2007; 102(6):2379–2388. (1985). [PubMed: 17289907]

Clarke AS, Lowell JE, Jacobson SJ, Pillus L. Esa1p is an essential histone acetyltransferase required for cell cycle progression. Mol. Cell. Biol. 1999; 19(4):2515–2526. [PubMed: 10082517]

Cotter TG. Apoptosis and cancer: the genesis of a research field. Nat. Rev. Cancer. 2009; 9(7):501–507. [PubMed: 19550425]

Fischer S, Wiesnet M, Renz D, Schaper W. H2O2 induces paracellular permeability of porcine brain-derived microvascular endothelial cells by activation of the p44/42 MAP kinase pathway. Eur. J. Cell Biol. 2005; 84(7):687–697. [PubMed: 16106912]

Gheldof A, Berx G. Cadherins and epithelial-to-mesenchymal transition. Prog. Mol. Biol. Transl. Sci. 2013; 116:317–336. [PubMed: 23481201]

Gomez-Bougie P, Menoret E, Juin P, Dousset C, Pellat-Deceunynck C, Amiot M. Noxa controls Mule-dependent Mcl-1 ubiquitination through the regulation of the Mcl-1/USP9X interaction. Biochem. Biophys. Res. Commun. 2011; 413(3):460–464. [PubMed: 21907705]

Guan D, Su Y, Li Y, Wu C, Meng Y, Peng X, Cui Y. Tetramethylpyrazine inhibits CoCl2 – induced neurotoxicity through enhancement of Nrf2/GCLc/GSH and suppression of HIF1alpha/NOX2/ROS pathways. J. Neurochem. 2015; 134(3):551–565. [PubMed: 25952107]

Huang LE, Gu J, Schau M, Bunn HF. Regulation of hypoxia-inducible factor 1alpha is mediated by an O2-dependent degradation domain via the ubiquitin-proteasome pathway. Proc. Natl. Acad. Sci. U. S A. 1998; 95(14):7987–7992. [PubMed: 9653127]

Jung DW, Kim WH, Seo S, Oh E, Yim SH, Ha HH, Chang YT, Williams DR. Chemical targeting of GAPDH moonlighting function in cancer cells reveals its role in tubulin regulation. Chem. Biol. 2014; 21(11):1533–1545. [PubMed: 25308277]

Kang J, Chen J, Shi Y, Jia J, Zhang Y. Curcumin-induced histone hypoacetylation: the role of reactive oxygen species. Biochem. Pharmacol. 2005; 69(8):1205–1213. [PubMed: 15794941]

Karakashev SV, Reginato MJ. Progress toward overcoming hypoxia-induced resistance to solid tumor therapy. Cancer Manage. Res. 2015; 7:253–264.

Kawamura T, Hasegawa K, Morimoto T, Iwai-Kanai E, Miyamoto S, Kawase Y, Ono K, Wada H, Akao M, Kita T. Expression of p300 protects cardiac myocytes from apoptosis in vivo. Biochem. Biophys. Res. Commun. 2004; 315(3):733–738. [PubMed: 14975762]

Kim JY, Ahn HJ, Ryu JH, Suk K, Park JH. BH3-only protein Noxa is a mediator of hypoxic cell death induced by hypoxia-inducible factor 1alpha. J. Exp. Med. 2004; 199(1):113–124. [PubMed: 14699081]

Kitajima Y, Miyazaki K. The critical impact of HIF-1a on gastric cancer biology. Cancers (Basel). 2013; 5(1):15–26. [PubMed: 24216696]

Lee SG, Lee H, Rho HM. Transcriptional repression of the human p53 gene by cobalt chloride mimicking hypoxia. FEBS Lett. 2001; 507(3):259–263. [PubMed: 11696352]

Liang T, Zhang X, Xue W, Zhao S, Pei J. Curcumin induced human gastric cancer BGC-823 cells apoptosis by ROS-mediated ASK1-MKK4-JNK stress signaling pathway. Int. J. Mol. Sci. 2014; 15(9):15754–15765. [PubMed: 25198898]

Lin MT, Kuo IH, Chang CC, Chu CY, Chen HY, Lin BR, Sureshbabu M, Shih HJ, Kuo ML. Involvement of hypoxia-inducing factor-1alpha-dependent plasminogen activator inhibitor-1 up-regulation in Cyr61/CCN1-induced gastric cancer cell invasion. J. Biol. Chem. 2008; 283(23): 15807–15815. [PubMed: 18381294]

Liu L, Ning X, Sun L, Zhang H, Shi Y, Guo C, Han S, Liu J, Sun S, Han Z, Wu K, Fan D. Hypoxia-inducible factor-1 alpha contributes to hypoxia-induced chemoresistance in gastric cancer. Cancer Sci. 2008; 99(1):121–128. [PubMed: 17953712]

Lowman XH, McDonnell MA, Kosloske A, Odumade OA, Jenness C, Karim CB, Jemmerson R, Kelekar A. The proapoptotic function of Noxa in human leukemia cells is regulated by the kinase Cdk5 and by glucose. Mol. Cell. 2010; 40(5):823–833. [PubMed: 21145489]

Luo HY, Wei W, Shi YX, Chen XQ, Li YH, Wang F, Qiu MZ, Li FH, Yan SL, Zeng MS, Huang P, Xu RH. Cetuximab enhances the effect of oxaliplatin on hypoxic gastric cancer cell lines. Oncol. Rep. 2010; 23(6):1735–1745. [PubMed: 20428833]

Matsunaga T, Tsuji Y, Kaai K, Kohno S, Hirayama R, Alpers DH, Komoda T, Hara A. Toxicity against gastric cancer cells by combined treatment with 5-fluorouracil and mitomycin c: implication in oxidative stress. Cancer Chemother. Pharmacol. 2010; 66(3):517–526. [PubMed: 19967538]

Oliveira MJ, Costa AM, Costa AC, Ferreira RM, Sampaio P, Machado JC, Seruca R, Mareel M, Figueiredo C. CagA associates with c-Met, E-cadherin, and p120-catenin in a multiproteic complex that suppresses Helicobacter pylori-induced cell-invasive phenotype. J. Infect. Dis. 2009; 200(5):745–755. [PubMed: 19604117]

Piret JP, Mottet D, Raes M, Michiels C. CoCl2, a chemical inducer of hypoxia-inducible factor-1, and hypoxia reduce apoptotic cell death in hepatoma cell line HepG2. Ann. N. Y. Acad. Sci. 2002; 973:443–447. [PubMed: 12485908]

Piret JP, Minet E, Cosse JP, Ninane N, Debacq C, Raes M, Michiels C. Hypoxia-inducible factor-1-dependent overexpression of myeloid cell factor-1 protects hypoxic cells against tert-butyl hydroperoxide-induced apoptosis. J. Biol. Chem. 2005; 280(10):9336–9344. [PubMed: 15611089]

Rankin EB, Giaccia AJ. The role of hypoxia-inducible factors in tumorigenesis. Cell Death Differ. 2008; 15(4):678–685. [PubMed: 18259193]

Rath S, Das L, Kokate SB, Pratheek BM, Chattopadhyay S, Goswami C, Chattopadhyay R, Crowe SE, Bhattacharyya A. Regulation of Noxa-mediated apoptosis in Helicobacter pylori-infected gastric epithelial cells. FASEB J. 2015; 29(3):796–806. [PubMed: 25404713]

Rath S, Anand A, Ghosh N, Das L, Kokate SB, Dixit P, Majhi S, Rout N, Singh SP, Bhattacharyya A. Cobalt chloride-mediated protein kinase Calpha (PKCalpha) phosphorylation induces hypoxia-inducible factor 1alpha (HIF1alpha) in the nucleus of gastric cancer cell. Biochem. Biophys. Res. Commun. 2016; 471(1):205–212. [PubMed: 26826385]

Rohwer N, Cramer T. HIFs as central regulators of gastric cancer pathogenesis. Cancer Biol. Ther. 2010; 10(4):383–385. [PubMed: 20647752]

Rohwer N, Lobitz S, Daskalow K, Jons T, Vieth M, Schlag PM, Kemmner W, Wiedenmann B, Cramer T, Hocker M. HIF-1alpha determines the metastatic potential of gastric cancer cells. Br. J. Cancer. 2009; 100(5):772–781. [PubMed: 19223895]

Sabharwal SS, Schumacker PT. Mitochondrial ROS in cancer: initiators, amplifiers or an Achilles' heel? Nat. Rev. Cancer. 2014; 14(11):709–721. [PubMed: 25342630]

Said HM, Hagemann C, Stojic J, Schoemig B, Vince GH, Flentje M, Roosen K, Vordermark D. GAPDH is not regulated in human glioblastoma under hypoxic conditions. BMC Mol. Biol. 2007; 8:55. [PubMed: 17597534]

Said HM, Polat B, Hagemann C, Anacker J, Flentje M, Vordermark D. Absence of GAPDH regulation in tumor-cells of different origin under hypoxic conditions in vitro. BMC Res. Notes. 2009; 2:8. [PubMed: 19144146]

Santer FR, Hoschele PP, Oh SJ, Erb HH, Bouchal J, Cavarretta IT, Parson W, Meyers DJ, Cole PA, Culig Z. Inhibition of the acetyltransferases p300 and CBP reveals a targetable function for p300 in the survival and invasion pathways of prostate cancer cell lines. Mol. Cancer Ther. 2011; 10(9): 1644–1655. [PubMed: 21709130]

Sullivan R, Graham CH. Hypoxia-driven selection of the metastatic phenotype. Cancer Metastasis Rev. 2007; 26(2):319–331. [PubMed: 17458507]

Tanaka T, Kitajima Y, Miyake S, Yanagihara K, Hara H, Nishijima-Matsunobu A, Baba K, Shida M, Wakiyama K, Nakamura J, Noshiro H. The apoptotic effect of HIF-1alpha inhibition combined with glucose plus insulin treatment on gastric cancer under hypoxic conditions. PLoS One. 2015; 10(9):e0137257. [PubMed: 26339797]

Torii S, Goto Y, Ishizawa T, Hoshi H, Goryo K, Yasumoto K, Fukumura H, Sogawa K. Pro-apoptotic activity of inhibitory PAS domain protein (IPAS), a negative regulator of HIF-1, through binding to pro-survival Bcl-2 family proteins. Cell Death Differ. 2011; 18(11):1711–1725. [PubMed: 21546903]

Urano N, Fujiwara Y, Doki Y, Tsujie M, Yamamoto H, Miyata H, Takiguchi S, Yasuda T, Yano M, Monden M. Overexpression of hypoxia-inducible factor-1 alpha in gastric adenocarcinoma. Gastric Cancer. 2006; 9(1):44–49. [PubMed: 16557436]

Vaupel P, Mayer A. Hypoxia in cancer: significance and impact on clinical outcome. Cancer Metastasis Rev. 2007; 26(2):225–239. [PubMed: 17440684]

Vaupel P. The role of hypoxia-induced factors in tumor progression. Oncologist. 2004; 9(Suppl. 5):10–17.

Wang G, Hazra TK, Mitra S, Lee HM, Englander EW. Mitochondrial DNA damage and a hypoxic response are induced by CoCl(2) in rat neuronal PC12 cells. Nucleic Acids Res. 2000; 28(10): 2135–2140. [PubMed: 10773083]

Wu D, Yotnda P. Induction and testing of hypoxia in cell culture. J. Vis. Exp. 2011

Xiao L, Kovac S, Chang M, Shulkes A, Baldwin GS, Patel O. Induction of gastrin expression in gastrointestinal cells by hypoxia or cobalt is independent of hypoxia-inducible factor (HIF). Endocrinology. 2012; 153(7):3006–3016. [PubMed: 22593272]

Xing F, Okuda H, Watabe M, Kobayashi A, Pai SK, Liu W, Pandey PR, Fukuda K, Hirota S, Sugai T, Wakabayshi G, Koeda K, Kashiwaba M, Suzuki K, Chiba T, Endo M, Mo YY, Watabe K. Hypoxia-induced Jagged2 promotes breast cancer metastasis and self-renewal of cancer stem-like cells. Oncogene. 2011; 30(39):4075–4086. [PubMed: 21499308]

Yang WY, Gu JL, Zhen TM. Recent advances of histone modification in gastric cancer. J. Cancer Res. Ther. 2014; 10(Suppl):240–245. [PubMed: 25693927]

Zhang L, Huang G, Li X, Zhang Y, Jiang Y, Shen J, Liu J, Wang Q, Zhu J, Feng X, Dong J, Qian C. Hypoxia induces epithelial-mesenchymal transition via activation of SNAI1 by hypoxia-inducible factor –1alpha in hepatocellular carcinoma. BMC Cancer. 2013; 13:108. [PubMed: 23496980]

Zhong H, De Marzo AM, Laughner E, Lim M, Hilton DA, Zagzag D, Buechler P, Isaacs WB, Semenza GL, Simons JW. Overexpression of hypoxia-inducible factor 1alpha in common human cancers and their metastases. Cancer Res. 1999; 59(22):5830–5835. [PubMed: 10582706]

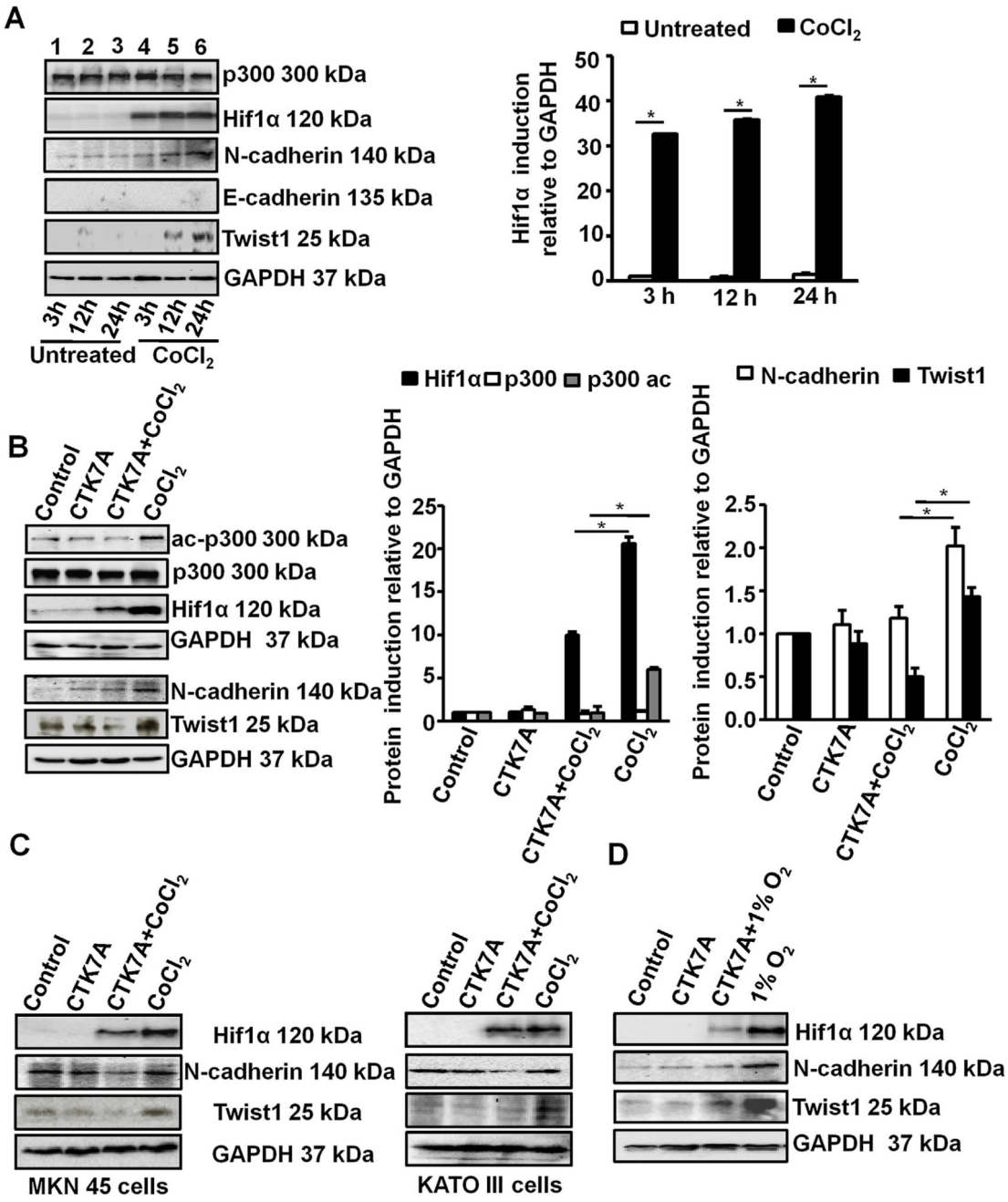

Fig. 1.

HAT inhibition downregulated $CoCl_2$ and 1% O_2-induced expression of metastatic markers in GCCs. (A) Expression of various metastatic factors was assessed at 3 h, 12 h, 24 h after treatment with 200 μM of $CoCl_2$ by western blotting (n = 3). GAPDH was used as a loading control. Graphical presentation of western blot data clearly showed significant induction of Hif1α from 3 h to 24 h of $CoCl_2$ treatment (mean ± SEM, n = 3), $*P < 0.05$. (B) Western blot analysis (n = 3) of whole cell lysates from AGS cells after treatment with 200 μM of $CoCl_2$ and/or 100 μM of CTK7A for 24 h. Bar diagrams represent status of EMT markers (mean ± SEM). $*P < 0.05$ (C) Western blot analysis (n = 3) indicated downregulation of

metastatic markers N-cadherin, Twist1, Hif1α in metastatic gastric cancer cell lines KATO III and MKN 45 after $CoCl_2$ and CTK7A treatment. (D) Western blot analysis (n = 3) of whole cell lysates from AGS cells after a hypoxia (1% O_2) exposure alone or with CTK7A. GAPDH was used as a loading control.

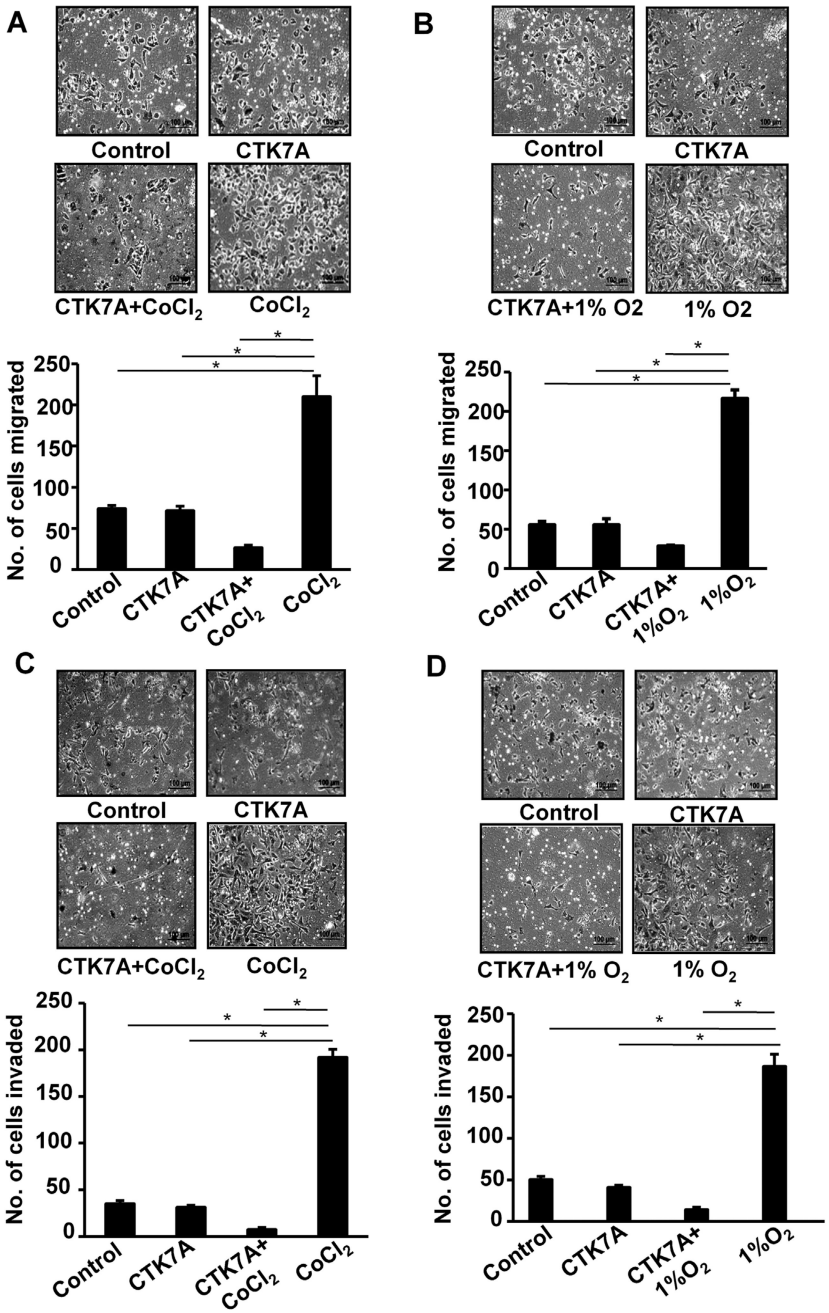

Fig. 2.

CTK7A reduced metastatic properties in $CoCl_2$-exposed and 1% O_2-treated GCCs. (A) AGS cells were suspended in serum-free media and were seeded onto upper chambers of 24 well inserts while lower chambers had 10% FBS-enriched media. After treatment, migrated cells were stained with haematoxylin and counted using an inverted microscope. Scale = 50 μm. Bars represent count of cells migrated from three independent experiments (n = 4, mean ± SEM). *$P < 0.05$. (B) AGS cells were treated with 1% O_2 alone or in combination with CTK7A (100 μM) or left untreated for 24 h and migration ability of these cells was assessed by counting the number of migrated cells (n = 4, mean ± SEM). *$P < 0.05$. Photographs

were taken using an inverted microscope equipped with camera (Primo Vert Carl Zeiss, Germany). Scale bar 200 μm. (C) Invasiveness of GCCs was studied by using matrigel-precoated Transwell after treatment with $CoCl_2$ (200 μM) alone or in combination with CTK7A (100 μM) for 24 h. Number of invading cells were stained with haematoxylin and counted (n = 4, mean ± SEM), $*P < 0.05$) by using an inverted microscope. (D) Invasiveness of GCCs was studied by using matrigel-precoated Transwell after treatment with 1% O_2 alone or in combination with CTK7A (100 μM) for 24 h. Invading cells were stained with haematoxylin and counted (mean ± SEM, n = 4, $*P < 0.05$) by using an inverted microscope.

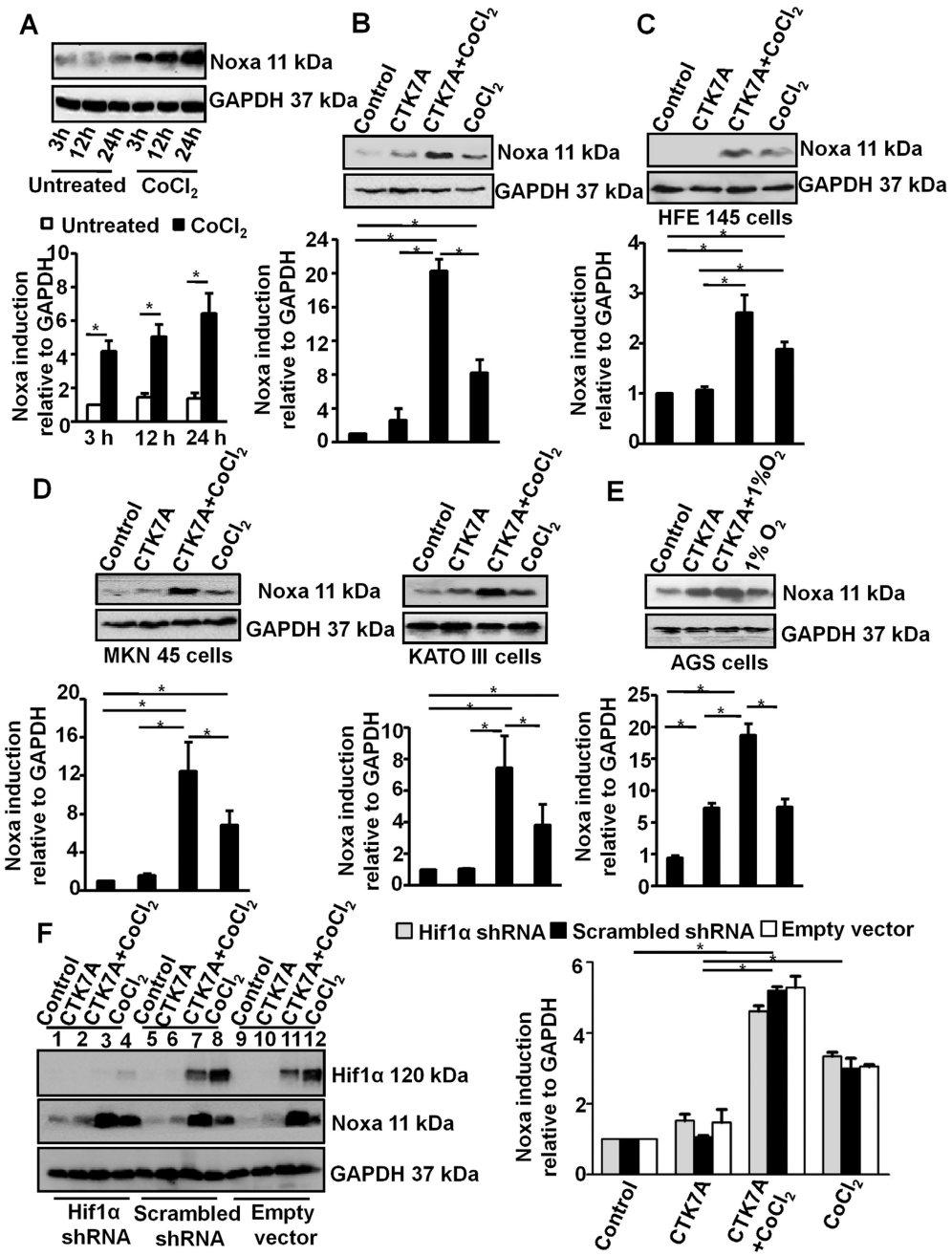

Fig. 3.

Inhibition of HAT induces Noxa expression in hypoxia-treated GCCs. (A) A representative western blot of whole cell lysates (n = 3) prepared from $CoCl_2$-treated (3 h, 12 h, 24 h with 200 μM of $CoCl_2$) AGS cells showed time-dependent induced expression of Noxa. GAPDH was used as a loading control. Graphical presentation of western blot data clearly indicated increment in Noxa expression with time (mean ± SEM, n = 3), $*P < 0.05$. (B) Expression of Noxa was analyzed by immunoblotting of cell lysates prepared from AGS cells treated with $CoCl_2$ (200 μM) and/or CTK7A (100 μM) for 24 h. GAPDH was used as a loading control. Graphical presentation of western blot data confirmed significant increase in Noxa

expression in CTK7A + $CoCl_2$-treated groups as compared to other groups (mean ± SEM, n = 3),* $P < 0.05$. (C) Immunoblot analysis of whole cell lysates prepared from immortalized human GCC HFE145 treated with $CoCl_2$ (200 μM) alone or in combination with CTK7A (100 μM) showed induced expression of Noxa in CTK7A + $CoCl_2$ combination treatment. GAPDH was used as a loading control. Bars depict Noxa expression normalized to GAPDH (mean ± SEM, $n = 3$), * $P < 0.05$. (D) Noxa expression in $CoCl_2$ (200 μM) and CTK7A (100 μM)-treated KATO III and MKN 45 cells. Analysis of data by Student's t-test clearly showed a significant increase in Noxa expression in CTK7A + $CoCl_2$-treated cells as compared to other groups. Bars represent mean ± SEM, $n = 3$, * $P < 0.05$. (E) Immunoblot analysis of whole cell lysates prepared from AGS cells treated with hypoxia (1% O_2) alone or in combination with CTK7A (100 μM) showed markedly induced expression of Noxa in CTK7A + hypoxia group. GAPDH was used as a loading control. (F) Immunoblot analysis (n = 3) showed equal expression of Noxa in the empty vector, scrambled negative control shRNA and Hif1α-shRNA stably-expressing AGS cells treated with 200 μM of $CoCl_2$ and/or CTK7A (100 μM) for 24 h. GAPDH was used as loading control. Data were further analyzed by 2-way ANOVA with Bonferroni *post hoc* test. Error bars, mean ±SEM. * $P <$ 0.05.

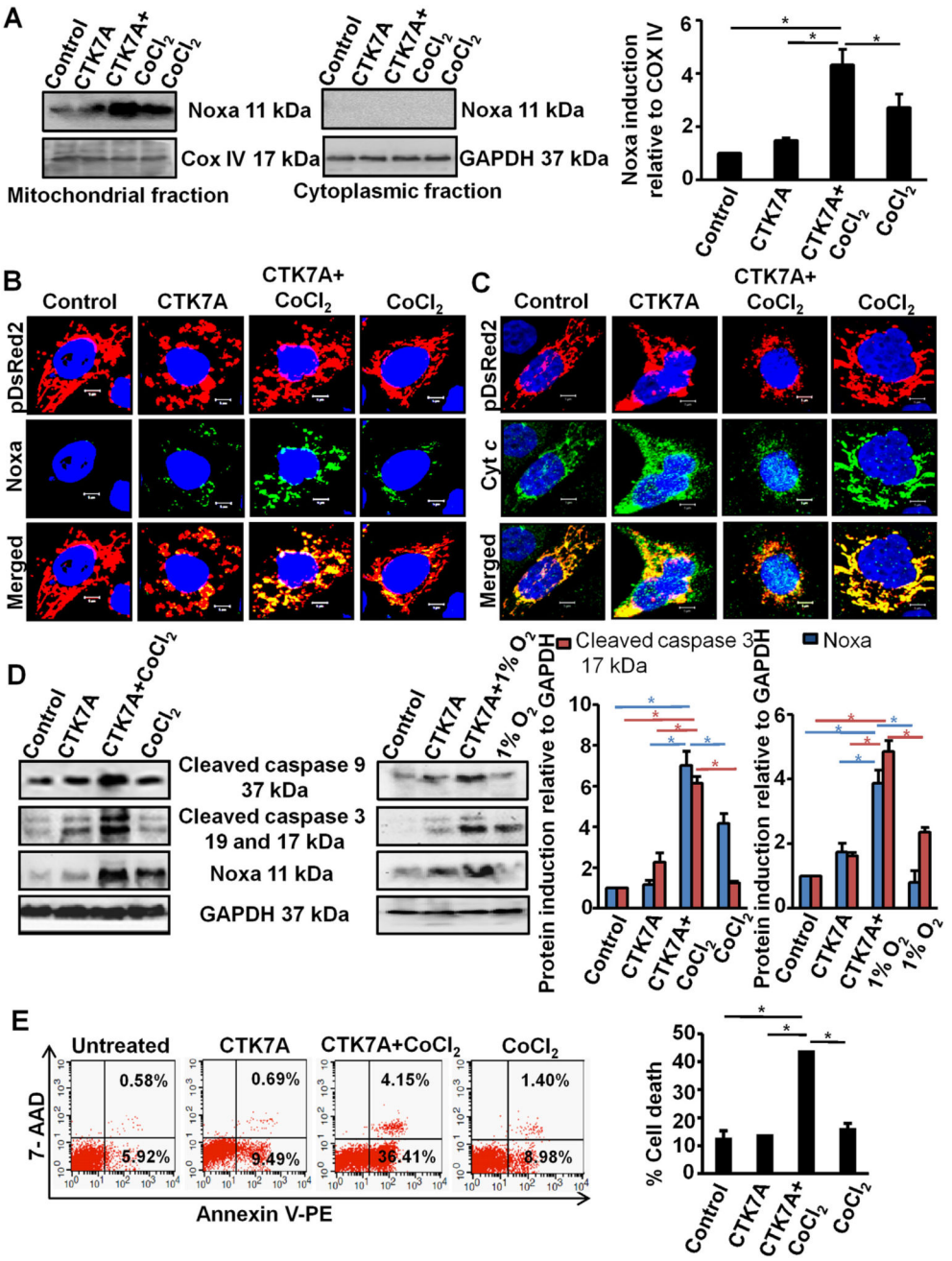

Fig. 4.

CTK7A induced intrinsic apoptosis by mitochondrial translocation of Noxa in $CoCl_2$-treated GCCs. (A) Western blot (n = 3) showing status of Noxa in the mitochondria and cytosolic fraction of AGS cells treated with $CoCl_2$, 200 μM, or in combination with CTK7A (100 μM) for 24 h. COX IV and GAPDH were used as loading controls for the mitochondrial and cytosolic fractions, respectively. Bars depict Noxa expression normalized to COX IV in the mitochondrial fraction (mean ± SEM, n = 3), $*P < 0.05$. (B) Confocal microscopy of AGS cells (n = 3) treated with $CoCl_2$ (200 μM) and/or CTK7A (100 μM) for 24 h showed high Noxa translocation to mitochondria in CTK7A + $CoCl_2$-treated cells. Nuclei were stained

with DAPI. Scale bar 10 μm. (C) Confocal microscopic image showing cytochrome *c* release from mitochondria in the above mentioned experimental groups. DAPI staining was for nucleus. Scale bar 10 μm. (D) Immunoblotting (n = 3) of whole cell lysates prepared from AGS cells after treatment with $CoCl_2$ (200 μM) or hypoxia (1% O_2) alone or in combination with CTK7A (100 μM) for 24 h indicated status of Noxa, cleaved caspase 3 and cleaved caspase 9. Error bars, mean ± SEM, $n = 3$,*$P < 0.05$. (E) AGS cells were treated with 200 μM $CoCl_2$ alone or in combination with CTK7A (100 μM) or left untreated. Cells were harvested and stained with Annexin V PE/7-AAD dyes. A representative dot plot (n = 4) indicated striking increase in apoptosis in CTK7A + $CoCl_2$-treated GCCs as compared to other treatment groups.% cell death were compared between various treatment groups (mean ± SEM, n = 4), *$P < 0.05$.

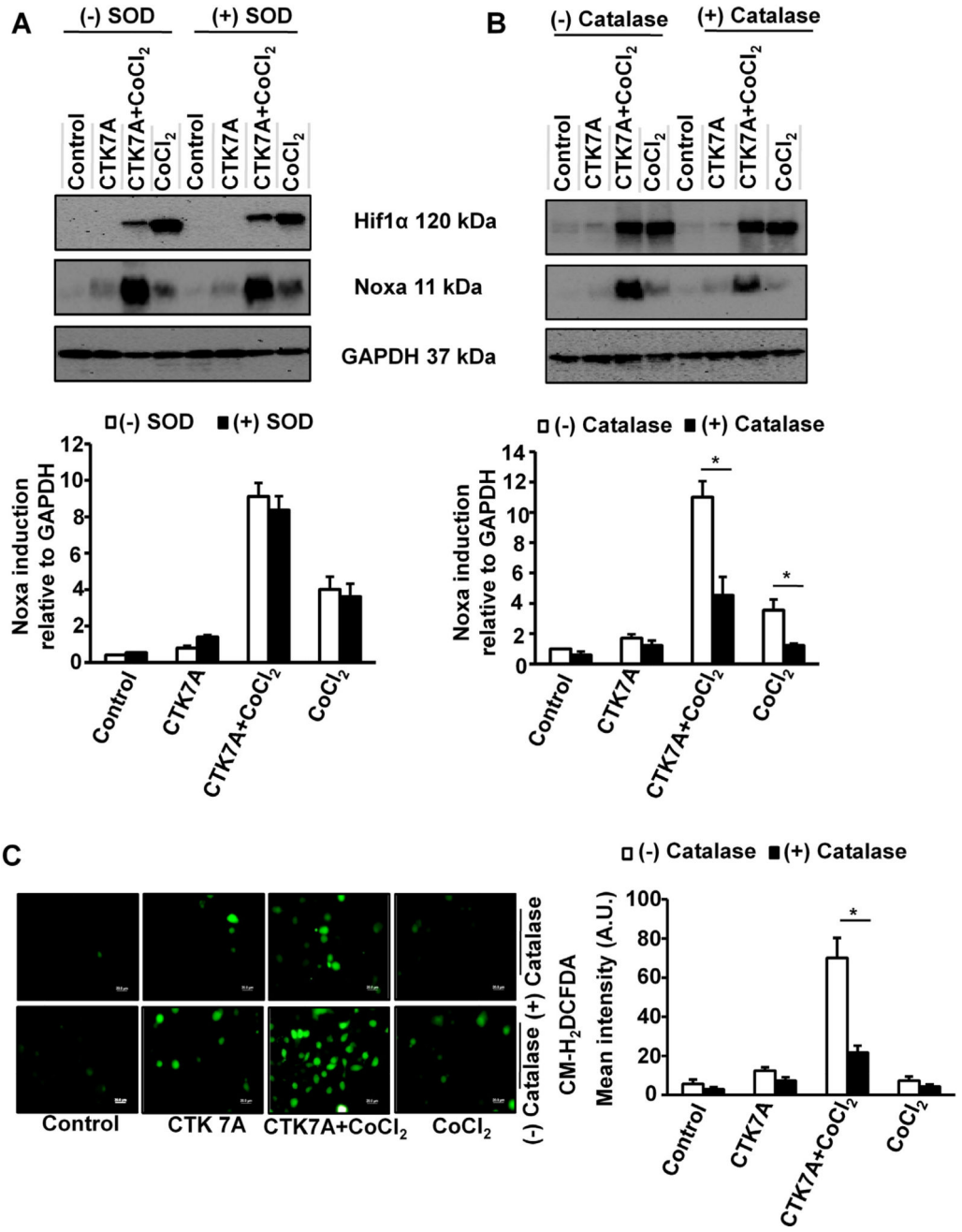

Fig. 5.

CTK7A-mediated increase in Noxa expression was regulated by ROS generation in $CoCl_2$-treated GCCs. (A) Immunoblot analysis (n = 3) of AGS cells after treatment with SOD for 4 h followed by treatment with $CoCl_2$ (200 μM) and/or CTK7A (100 μM) for detection of Noxa and Hif1α expression. GAPDH was used as a loading control. Bars depict Noxa expression normalized to GAPDH (mean ± SEM, n = 3), $*P < 0.05$. (B) Western blotting (n = 3) of cell lysates after treatment with catalase (350 units/ml) for 4 h followed by above mentioned combination of CTK7A and $CoCl_2$ for detection of Noxa and Hif1α expression. Graphical presentation of Noxa expression was shown by bar diagrams (mean ± SEM, n =

3), *$P < 0.05$. (C) AGS cells were treated with $CoCl_2$ (200 μM) alone or in combination with CTK7A (100 μM) for 24 h with or without catalase pre-treatment (350 units/ml, 4 h). Cells were then incubated with fluorescence probe CM-H_2DCFDA at a final concentration of 1 μM for 10 min followed by fixation with paraformaldehyde at 37°C for 20 min. ROS generation was measured under a fluorescence microscope (Olympus, Japan). Scale bar, 20 μm. Bars depict mean fluorescence intensity (mean ± SEM, n = 3), *$P < 0.05$.

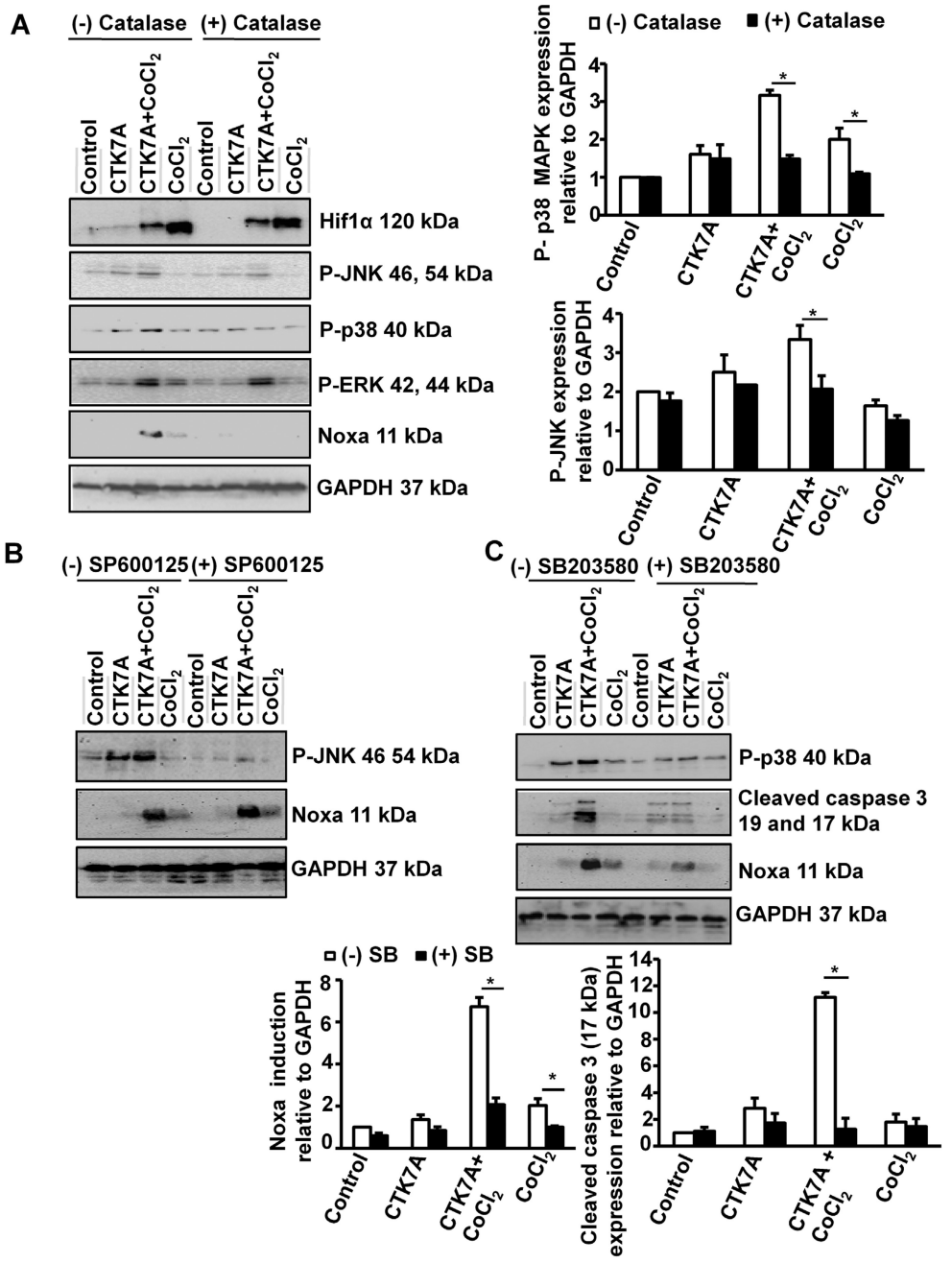

Fig. 6.

CTK7A induced p38 MAPK phosphorylation and Noxa upregulation via generation of H_2O_2 in $CoCl_2$-treated GCCs. (A) Western blot analysis (n = 3) of whole cell lysates from AGS cells pre-treated with catalase (350 units/ml) for 4 h followed by treatment with 200 μM of $CoCl_2$ alone or in combination with CTK7A for 24 showed effect of ROS on Noxa, Hif1α and all MAPKs. Bar diagrams represent status of p38 MAPK and JNK (mean ± SEM, n = 3) *$P < 0.05$. (B) Western blotting (n = 3) showed the status of P-JNK and Noxa after pre-treatment with 25 μM JNK inhibitor II (SP600125) for 1 h followed by $CoCl_2$ (200 μM) and/or CTK7A (100 μM) treatment for 24 h. GAPDH was used as a loading control. (C)

Immunoblotting (n = 3) of AGS cell lysates showed the effect of p38 MAPK inhibition on cleaved caspase 3 and Noxa after pre-treatment with 25 μM p38 MAPK inhibitor (SB203580) for 1 h followed by $CoCl_2$ (200 μM) treatment and/or CTK7A (100 μM) for 24 h. Graphs depict expression pattern of Noxa and cleaved caspase 3 normalized to GAPDH (mean ± SEM, n = 3), $*P < 0.05$.